

## Impedance Spectroscopic and Phase Transition Study of A New Organic – inorganic Alkali Earth Hybrid

M. F. Mostafa\*, A. K. Tammam and Dina Gawad#

Physics Department, Faculty of Science, Cairo University, Giza, Egypt

**T**HE NEW ORGANIC–inorganic hybrid 1,7-heptanediammonium-calcium tetrachloride, with molecular formula  $[(\text{CH}_2)_7(\text{NH}_3)_2] \text{CaCl}_4$ , crystallized in a monoclinic Pm space group,  $a = 4.625 \text{ \AA}$ ,  $b = 11.205 \text{ \AA}$ ,  $c = 12.391 \text{ \AA}$ ,  $\alpha = 90^\circ$ ,  $\beta = 86.82^\circ$ ,  $\gamma = 90^\circ$ ,  $V = 641.2 \text{ \AA}^3$ , density =  $1.63 \text{ mgm}^{-3}$  and  $Z = 2$ . Differential thermal scanning of the new organic–inorganic hybrid showed five phase changes; chain melting transitions at  $T_1 = 329.2 \text{ K}$  and  $T_2 = 326.49 \text{ K}$  and three transitions at  $T_3 = 283.6 \text{ K}$ ,  $T_4 = 278.8 \text{ K}$  and  $T_5 = 260.8 \text{ K}$  associated with solid–solid phase changes. Permittivity and ac conductivity as a function of temperature (170 K– 425 K) and frequency (0.06 kHz <  $f$  < 40 kHz) are presented. Bulk conductivity behavior is thermally activated. Three temperature regions where conductivity is thermally activated were identified. The frequency dependent activation energy in the two temperature regions (355–423 K and (243– 261) K are  $\Delta E_{(i)} = 0.64\text{--}0.42 \text{ eV}$  and  $\Delta E_{(ii)} = 1.75\text{--}0.42 \text{ eV}$  respectively. In phase (III)  $\Delta E_{(iii)} = 4.44 \times 10^{-4} \text{ eV}$  and is frequency independent.

**Key words:** Thermal properties, Dielectric properties, AC conductivity

### Introduction

Recently, organic-inorganic halide perovskite hybrids (OIHs) are being thoroughly investigated mainly because of their interesting dielectric properties, optoelectronic characteristics, as well as their several consecutive structural phase transformations that have direct effect on their dielectric properties and transport mechanism [1]. The two dimensional layered perovskite hybrids  $A_2MX_4$  where A = alkylammonium or alkylenediammonium, M = divalent transition metal ion, X = Cl/Br/I, have been thoroughly studied for their interesting magnetic properties and well as their intriguing structure phase transformations [2,3]. Besides they are excellent models [3]. Being solids, they make excellent candidates to study their properties by solid state techniques. Most previous studies were concerned with A being alkyl monoammonium and M is a divalent transition metal ion e.g.  $\text{Mn}^{2+}$ ,  $\text{Fe}^{2+}$ ,  $\text{Co}^{2+}$ ,  $\text{Cu}^{2+}$ ,  $\text{Zn}^{2+}$  and  $\text{Cd}^{2+}$ . where the metal is tetrahedrally or octahedrally coordinated with the halide ion. From a structural point of view, hybrids with M = Co [4] and Zn [5] consist of layers of isolated  $\text{MX}_4$  tetrahedra alternating with organic layers of the chains.

These differ from those where M = Mn [6], Fe [7], Cu [8] and Cd [9] which consist of two dimensional networks of corner sharing  $\text{MX}_6$  octahedra alternating with chain layers. The difference in the packing of the aliphatic part is relevant since it governs the sequence of phase transitions. The sequence of transitions depends on the number of carbon atoms/chain which has been correlated with packing characteristics [10]. Replacement of transition metal ions in  $A_2MX_4$  hybrid by the biologically important Ca (II) or Mg (II) is likely to shed some light on the conduction mechanisms in biological systems. Hence, the study of complexes formed with alkylenediammonium and Ca halide using impedance spectroscopy will provide valuable information about electric transport in these OIH as a model of lipids. In this article we present preparation, characterization, thermal properties and impedance spectroscopic study of the new long chain  $[(\text{CH}_2)_7(\text{NH}_3)_2] \text{CaCl}_4$ .

### Experimental

The material was prepared by mixing 1,7-diammonium chloride and calcium chloride alcoholic solutions in a 1:1 ratio. The mixture was heated for one hour at  $70^\circ \text{C}$  and cooled gradually

\*Corresponding author: e-mail: mohga40@yahoo.com

#In Partial fulfillment of M.Sc. Degree

DOI :10.21608/ejphysics.2018.3562.1001

©2018 National Information and Documentation Center (NIDOC)

to room temperature. Colorless crystallites were formed. They were washed then re dissolved in ethanol and recrystallized twice.

Elemental analysis was carried out at the microanalysis unit at the University of Cairo. The elemental analysis showed the percent of carbon =26.62% (26.764%) and hydrogen =6.28% (6.417%); theoretical values are given in brackets.

IR spectra between 4000 and 200  $\text{cm}^{-1}$  were obtained on an FTIR 5000 spectrometer at the microanalysis unit at the University of Cairo using KBr pellet under a pressure of 0.5 ton/ $\text{cm}^2$ . The results of elemental analysis and IR spectra confirmed the formation of the desired material, namely  $[(\text{CH}_2)_7(\text{NH}_3)_2] \text{CaCl}_4$ , henceforth 7CaC. Table 1 lists IR bands ( $\text{cm}^{-1}$ ) and their assignments of 7CaC sample at room temperature.

**TABLE 1. IR bands ( $\text{cm}^{-1}$ ) and their assignments of 7CaC sample at room temperature.**

IR bands [ $\lambda$ ( $\text{cm}^{-1}$ )]	Assignment
3388, 3037	$\nu_{\text{as}}(\text{NH}_3)^+$
2932 (m)	$\nu_{\text{s}}(\text{NH}_3)^+$
2864	$\delta_{\text{s}}(\text{CH}_2)$ , N-H...Cl
1594 (s)	$\delta_{\text{as}}(\text{NH}_3)^+$
1472 (s)	$\delta_{\text{s}}(\text{NH}_3)^+$ $\delta_{\text{as}}(\text{CH}_2)$
1402 (w)	$\delta, \omega(\text{CH}_2)$
	$\delta, \rho(\text{CH}_2)$
1281 (m)	$\nu(\text{C-C})$ , $\rho(\text{CH}_2)$
1170, 1136	$\rho(\text{CH}_2)$
	$\rho(\text{C-C})$ , $\nu(\text{CH}_2)$
1037	$\nu(\text{C-H})$
1007	$\Delta(\text{C-C-N})$
944, 887	$\nu(\text{C-N})$ , $\nu(\text{C-C})$ , $\rho(\text{NH}_3)^+$
774, 727	$\rho(\text{CH}_2)$
590	$\nu(\text{C-Cl})$
412	$\delta(\text{C-C-N})$ , $\delta(\text{C-C})$ $\tau(\text{NH}_3)^+$ $\delta(\text{Ca-Cl})$
	Liberation

For bands: sh= sharp, s= strong, m= medium, w= weak.

For assignment:  $\nu_{\text{as}}$  = asymmetric stretching,  $\nu_{\text{s}}$  = symmetric stretching,  $\delta_{\text{as}}$  = asymmetric deformation,  $\delta_{\text{s}}$  = symmetric deformation,  $\Delta$  = bending,  $\rho$  = rocking,  $\omega$  = wagging,  $\tau$  = torsion.

Differential thermal scanning (DSC) measurements were carried out on a Shimadzu differential thermal scanner analyzer model DSC-60 at a scanning rate 5 °C/min. Powdered crystals weighing 2.5 mg were used. Measurements were performed under a stream of dry nitrogen gas at a rate of 50 ml/min. The thermograph was calibrated with the melting transition of Indium at 157 °C.

Impedance spectroscopic measurements using a computer controlled lock-in amplifier type SR830 was carried out under nitrogen atmosphere using samples in the form of compressed pellets of 6.0 mm in diameter and 1.0mm thick. Samples were coated with Ag paste to ensure good electrical contact. Temperature was measured using a copper constantan thermocouple. The temperature was controlled between 170 K-425 K with stability 0.5 K. Measurements were carried out in the frequency range 60 Hz–40 kHz in an applied potential of 1 V.

## Results and Discussion

### Powder x-ray

Room temperature x-ray powder diffraction of 7CaC is depicted in Fig.1. Table 2 lists observed and calculated  $2\theta$  values of 7CaC values and h k l assignments. Using Treor [11] and Chekcell [12] indexing programs, the best solution was found to be monoclinic system (sp.gr. Pm) with  $a=4.625 \text{ \AA}$ ,  $b= 11.205 \text{ \AA}$ ,  $c= 12.391 \text{ \AA}$  and  $\beta= 86.82^\circ$ ,  $Z= 2$ ,  $d= 1.63 \text{ gm/cm}^3$ ,  $V= 641.2 \text{ \AA}^3$ .

### Thermal analysis

The DSC thermograph for the sample in the temperature range ( $240 \leq T \text{ (K)} \leq 400$ ), is shown in

Fig. 2. Table 3 lists the transition temperatures and the corresponding entropy values. Five peaks are observed in the temperature range 240 K- 340 K. Starting from the high temperature side, The first two consecutive peaks  $T_1= 329.3$  and  $T_2= 326.5$  are manifestation of chain melting transitions typical of layered type diammonium metal halide pervoskites [13, 14]. Chain melting transitions are characterized by a major peak having large entropy value followed or preceded by the minor peak having smaller entropy. The major peak is associated with the different sequence of trans-gauche conformations of the chains. The minor is related to orientation of the chains among equilibrium positions. At this transition the space group and the interlayer spacing change and the chain undergoes rapid motion [13]. In the low temperature regime three transitions are observed. A well defined  $\lambda$ - like transitions at  $T_5= 260.8 \text{ K}$  typical of first order phase change is likely to be due to commensurate- incommensurate phase change. A second peak at  $T_4= 278.8 \text{ K}$  is likely be due to incommensurate-unmodulated phase transition has a long tail on the low temperature side followed by a very small anomaly at  $T_3= 283.6 \text{ K}$  as seen in insert (i). Transition ( $T_5$ ) is likely to involve distortion of the metal-halide octahedron.

### Dielectric constant results

#### Temperature dependent dielectric constant

Dielectric measurement was performed in the temperature range 170 K- 425 K. Temperature independent behavior was observed in the range 170 K-225 K and will not be shown. For clarity, the real part of the dielectric constant ( $\epsilon'$ ) of 7CaC as a function of temperature in the range

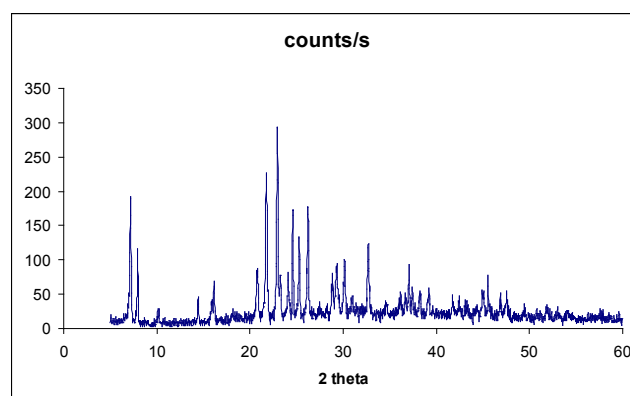


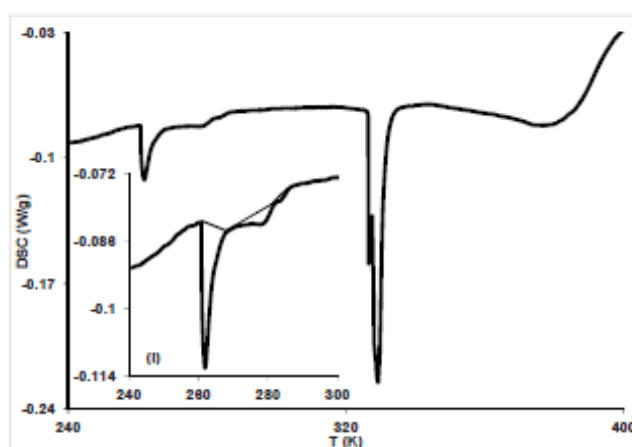
Fig. 1. Room temperature x-ray powder diffraction pattern of 7 CaC.

**TABLE 2. XRD (h k l) assignments, observed, calculated and difference of  $2\theta$  values of 7CaC at room temperature.**

$N_{\theta}$	H	k	L	$2\theta_{\text{Obs}}(^{\circ})$	$2\theta_{\text{cal}}(^{\circ})$	$\Delta\theta(^{\circ})$
1	0	0	1	7.205	7.145	0.060
2	0	1	0	7.955	7.890	0.065
3	0	0	2	14.435	14.318	0.117
4	-1	1	0	20.795	20.805	0.010
5	1	1	1	21.725	21.668	0.057
6	0	1	3	22.955	22.979	0.024
7	1	0	2	23.375	23.391	0.016
8	-1	0	2	24.575	24.689	0.114
9	-1	2	1	26.255	26.321	0.066
10	0	0	4	28.865	28.865	0.000
11	1	1	3	29.315	29.328	0.013
12	0	1	4	30.035	29.970	0.065
13	-1	1	3	30.875	30.909	0.034
14	0	4	1	32.795	32.779	0.016
15	-1	3	2	34.535	34.575	0.040
16	-1	1	4	36.755	36.774	0.011
17	0	1	5	37.175	37.212	0.037
18	0	3	4	37.745	37.763	0.018
19	1	4	1	38.135	38.063	0.072

**TABLE 3. DSC transition temperatures and corresponding entropy of 7CaC.**

	$T_5(\text{K})$	$T_4(\text{K})$	$T_3(\text{K})$	$T_2(\text{K})$	$T_1(\text{K})$
$T_{\text{onset}}(\text{K})$	260.8	275.4	282.6	326.2	327.6
$T_{\text{peak}}(\text{K})$	261.8	278.8	283.6	326.5	329.3
$\Delta S(\text{J/mol.K})$	2.09	0.17	0.02	0.88	4.81

**Fig. 2. DSC thermograph in the temperature range (240 - 400) K.**

225 K- 425 K is shown in Fig. 3. a. A frequency dependent asymmetric peak is noted with a pronounced shoulder on the high temperature side, a peak maximum at  $T \sim 266$  K that decreases exponentially with frequency. The peak is not annihilated at the maximum attained frequency of 40 kHz. A frequency dependent shoulder at  $T \sim 281$  K, of much lower magnitude appears on the high temperature side as seen in the insert (i). As temperature increases a broad hump could be identified as two consecutive shallow peaks located at 327 K and 333 K, which can be associated with the DSC transitions  $T_2$  and  $T_1$  respectively. A shift of the peaks' maxima by  $\sim 4$ -5 K to higher temperatures compared to DSC transition temperatures is observed. This is ascribed to the difference in the heating rates of the two measuring techniques. Both peaks are frequency independent.

The imaginary part of the dielectric constant of 7CaC is shown in Fig. 3.b. Similar behavior to that of  $(\epsilon')$ , except for a much higher  $(\epsilon'')$  values of  $T_4$ -peak but smaller  $(\epsilon'')$  magnitude for the other peaks, see insert (ii).

*Frequency dependent dielectric constant*

Variation of the complex dielectric constant  $[\ln(\epsilon^*)]$  as a function of frequency, at several

selected temperatures, is shown in Fig. 4.a. For the frequency range,  $f < 60$  Hz, space charges predominates. Above that frequency, the real part of the dielectric constant  $[\ln(\epsilon')]$  vs.  $[\ln(\omega)]$  shows a decreasing dielectric constant with increasing frequency. A normal behavior is the rise of the dielectric constant with increasing temperature which is clearly seen in Fig. 3.a The Variation of  $\ln \epsilon'$  vs.  $\ln \omega$  is approximated by the relationship

$$\epsilon^* \propto \omega^{-\nu} \tag{1}$$

Variation of  $n_1 = [d(\ln(\epsilon')) / d(\ln(\omega))]$  is calculated. Plot of  $n_1 = [d(\ln(\epsilon'))] / [d(\ln(\omega))]$  as a function of temperature is shown in Fig 4. b. It reveals the large drop in  $n_1$  at  $T = 250$  K-280 K and the small anomalous change at  $T = 323$  K- 333 K confirming the phase transitions, as shown in the insert (i). The variation of  $[\ln(\epsilon'')]$  vs.  $[\ln(\omega)]$  is shown in Fig. 4.c. An important feature is the gradual decrease of  $[\ln(\epsilon'')]$  to a shallow minimum with increasing frequency. The minimum shifts to higher frequencies as temperature increases. This  $(\epsilon'' - \omega)$  behavior has been observed in many disordered materials and is associated with change from universal dielectric response (UDR) to superlinear power law (SLPL) [15, 16].

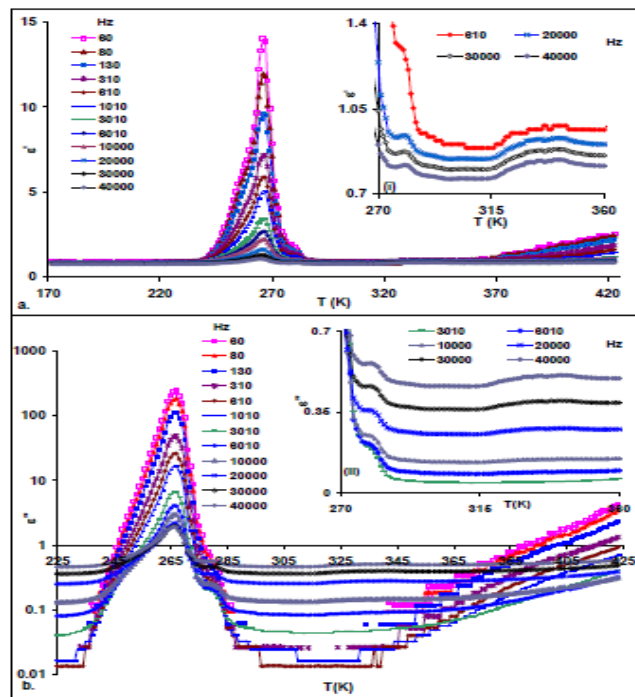


**Fig. 3. a:** Real part of dielectric constant ( $\epsilon'$ ) vs.  $T(K)$  at selected frequencies. **Insert (i):** Real part of the dielectric constant ( $\epsilon'$ ) vs.  $T(K)$  in the range (270- 360) K at several frequencies. **b:** Imaginary part of dielectric constant ( $\epsilon''$ ) vs.  $T(K)$ , at selected frequencies, on log scale. **Insert (ii):** ( $\epsilon''$ ) vs. temperature in the range (270- 360) K at several frequencies.

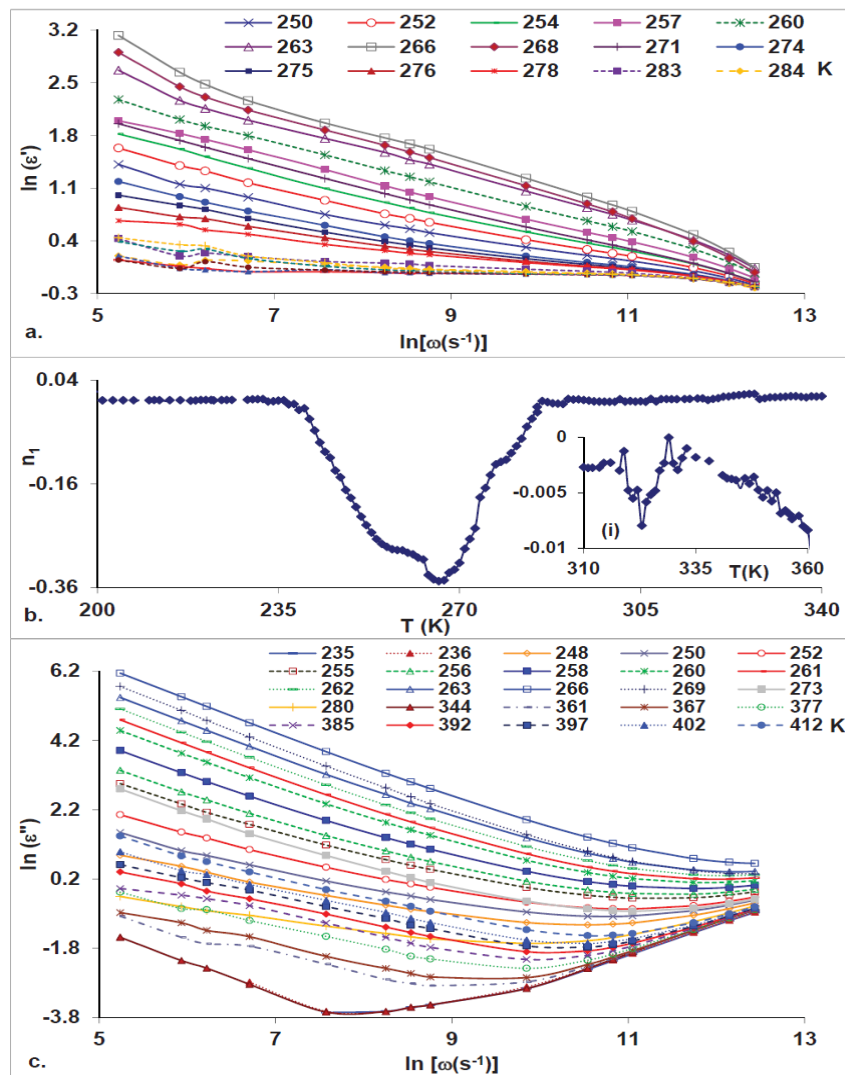


Fig. 4. Fig. 4.a: Real part of dielectric constant vs. angular frequency [ $\ln(\epsilon')$  vs.  $\ln(\omega(\text{s}^{-1}))$ ] at selected temperatures. b:  $n_1 = d[\ln(\epsilon')]/d[\ln(\omega)]$  vs. temperature in the temperature range (200-340) K. (i):  $n_1$  vs. temperature on enlarges  $n_1$ -scale in the temperature range (310-360) K. c: Imaginary part of dielectric constant vs. angular frequency [ $\ln(\epsilon'')$  vs.  $\ln(\omega(\text{s}^{-1}))$ ] at selected temperatures.

### Conductivity results

#### Temperature dependent conductivity

Figure 5a shows the variation of the conductivity as a function of reciprocal temperature [ $\ln(\sigma)$  vs.  $(1000/T)$ ] at different frequencies. Three temperature regions were identified where Arrhenius relation holds corresponding to phases I, II and III in the temperature ranges ( $T > 355$  K), ( $243 < T(\text{K}) < 261$ ) and ( $T < 235$  K) respectively. The intermediate temperature range ( $266 < T(\text{K}) < 355$ ) where Arrhenius relation does not hold is denoted (IT). Conductivity temperature and frequency dependence is different in the different phases. In phases (I), and (II) the conductivity

is thermally activated, following Arrhenius type relation:

$$\sigma = A_0 e^{-\Delta E/kT} \quad (2)$$

$A$  is pre-exponential factors,  $\Delta E$  is the activation energy,  $k$  is the Boltzmann constant and  $T$  is the absolute temperature. Variation of the activation energy in the two regions were fitted to the relation

$$\Delta E = \Delta E_0 [1 - \exp(-f_0/f)^\alpha] \quad (3)$$

as shown in Fig. 5.b. The fit parameters are listed in Table 4. In phase (III) at temperatures below 235 K, conductivity is temperature independent but strongly dependent on frequency, indicating extrinsic type conduction.

The value of  $\Delta E \sim 0.6$  eV (phase I) which is in agreement with values previously obtained for similar OIH and is typical of  $\text{Cl}^-$  vacancy conduction mechanism and suggests that hopping of chloride ion may be responsible for the conduction in the high temperature range [4, 5, 17]. This is as would be expected where at high temperatures  $[\text{CaCl}_4]^{2-}$  anion acquires enough energy to orient, and that the N-H...Cl bonds weakens, which would result in hopping of  $\text{Cl}^-$  ion among vacant sites.

In phase (II),  $243 < T(\text{K}) < 261$ , the activation energy is frequency dependent, decreases with increasing frequency. It is more than twice as large

as that of phase (I). This is not surprising since the large activation energy is calculated within the temperature range of the phase transition range, where  $\text{Cl}^-$ , protons as well as chain librations contribute to the conduction.

Considering the structural characteristics of the sample, conduction is related to movement of the ammonium group and its relation to the hydrogen bonding with the chloride ion. It is likely that as the hydrogen bond breaks, simultaneous jump of chloride ions and of protons among vacant sites takes place. Also as the N-H...Cl bonds weakens, correlated orientation of the organic chains are facilitated.

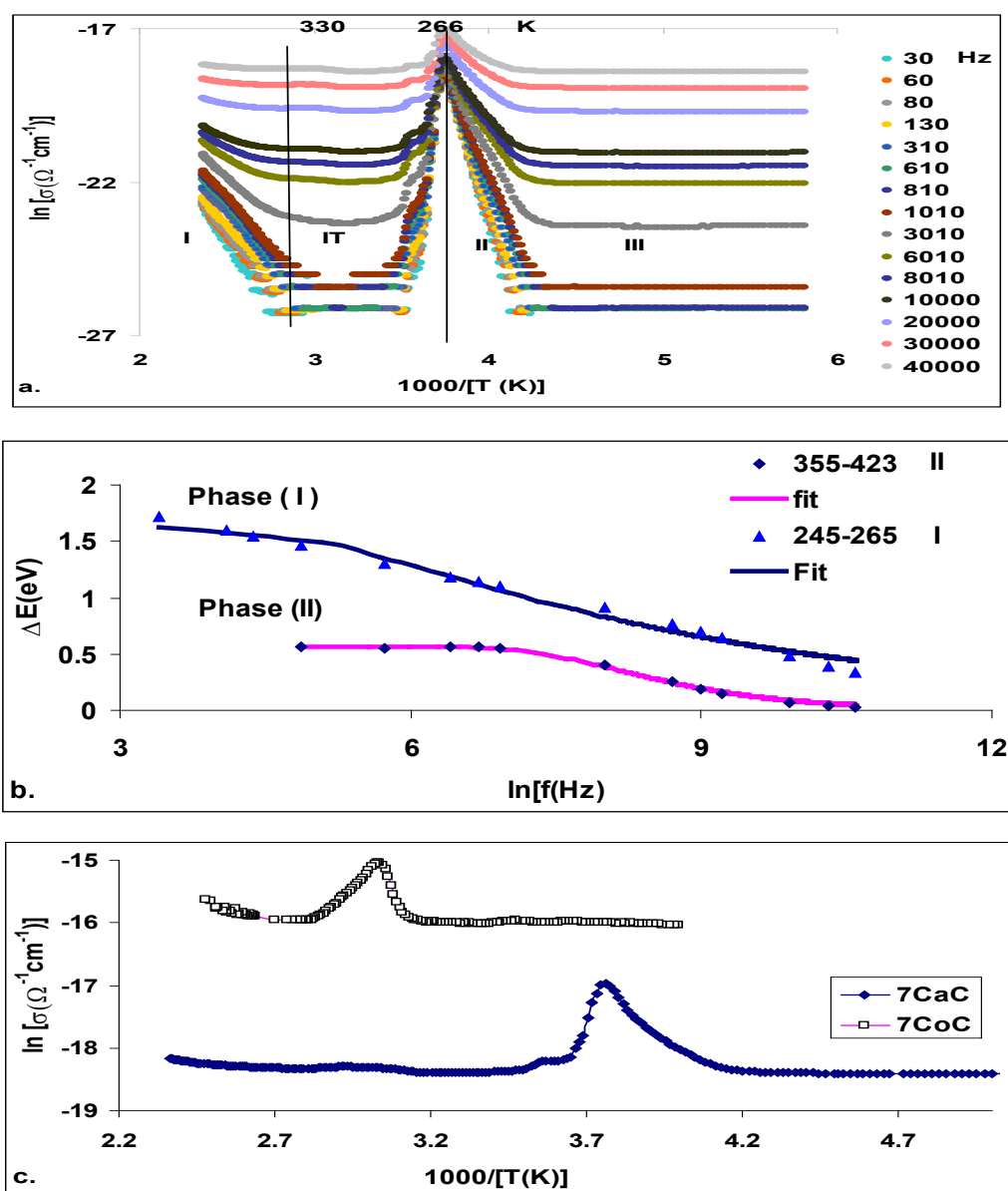


Fig. 5. Fig. 5.a: AC conductivity vs. reciprocal temperature:  $\ln(\sigma(\Omega.\text{cm})^{-1})$  vs.  $1000/[T(\text{K})]$  at different frequencies. b: Activation energy as function of frequency:  $\Delta E$  (eV) vs.  $[\ln(f(\text{Hz}))]$  and its fit. c:  $\ln[\sigma(\Omega.\text{cm})^{-1}]$  vs.  $1000/T(\text{K})$  at 40 kHz for 7CaC and 7CoC.

**TABLE 4. Activation energy  $\Delta E$  (eV) in the different temperature ranges and its fit parameters according to Eq.7.**

Temperature range (K)	Phase	$\Delta E$ (eV)	$\Delta E_0$ (eV)	$f_0$ (Hz)	$\alpha$
(366- 423)	(I)	0.64-0.42	0.625± 0.004	3117± 220	1.00± 0.054
(243- 261)	(II)	1.75-0.42	1.722± 0.020	147.4± 16.5	0.24± 0.007
( T < 235)	(IV)	Frequency independent with $\Delta E_0 = 4.44 \times 10^{-4}$ eV			

Figure 5c displays conductivity vs.  $1000/T$  at 40 kHz of  $7CaC$  and the corresponding  $[(CH_2)_7(NH_3)_2]CoCl_4$ , denoted  $7CoC$  [17] respectively for comparison. It is interesting to note that while conductivity values indicates that  $7CaC$  is an insulator, (maximum value of  $\sigma \sim 10^{-8} (\Omega.cm)^{-1}$  at 266 K), whereas conductivity of  $7CoC$  is in the semiconductor range ( $\sigma \sim 2 \times 10^{-7} (\Omega.cm)^{-1}$ ). This could be attributed to the size of the metal ion as well as its electronic characteristics such as the electronegativity. The metal ion size is related to the distortion of the metal halide octahedron or tetrahedron (while electronegativity influences the metal halide bond strength and bond length. It is also noticed that the two hybrids show phase transitions such that the transition temperatures shift to higher values as the metal ion changes.

### Conclusion

The hybrid shows peculiar phase transitions at low temperature and the usual chain melting transitions above room temperature, that are reflected in the dielectric measurements. Comparison to OIH where the metal ion belongs to the transition metal group showed much lower conductivity values. Activation energy is frequency dependent and differ in the different phases. At high temperature ( $T > 355$  K),  $Cl^-$  ion hopping with  $\Delta E = 0.6$  eV prevails. In the low temperature range ( $T < 267$  K)  $\Delta E$  is nearly twice as large, this is not surprising since the large activation energy is calculated within the temperature range of the phase transition, where  $Cl^-$ , protons as well as chain librations contribute to the conduction.

### References

- Zhao, Y and Zhu, K., *Chem. Soc. Rev.* **45** (2016) 655.
- De Jongh, L.J. and Miedema, A.R., *Adv. Phys.* **23** (1974)
- Ruiz-Hitzky, E., *The chemical Record*, **3** (2003)
- Mostafa, M. F., El Aal, S. K. and Tammam, A.K., *Ind. J. Phys.* **88** (2014) 49.
- Mostafa, M. F. and El Khiyami, S. *J. Sol. St. Chem.* **209** (2014) 82
- Guillaume, F., Sourisseau, C. and Dianoux, A. J. , *J. Phys. Chem.*, **94** (1990) 3438.
- Willett, R.D. and Riedel, F.E., *Chem. Phys.* **7** (1975)112.
- Garland, J., Emerson, K. and Pressprich, M., *Acta Cryst.* **C46** (1990) 1603.
- Khechoubi, M., Bendani, A., Chanh, N., Courceille, C. Duplessix and Couzis, M., *J. Phys. Chem. Sol.* **55** (1994) 1277.
- Zuniga, F. J. and Chapuis, G., *Acta Cryst.*, **839** (1983) 620.
- Werner, P.E., Eriksson, L. and Westdahl, M., *J. Appl. Cryst.* **18** (1985) 367.
- Laugier, J. and Bochu, B., Checkcell distributed free from the CCP14; website: [http:// www.ccp14.ac.uk/tutorial/lmgp/](http://www.ccp14.ac.uk/tutorial/lmgp/)
- Kind, V, Plesko, S., Gunter, P., J. Roos, Fousek, J., *Phys. Rev.* **B23** (1981) 5301.
- Gomez Cuevas, A., Tello, M. and Lopez Echarri, A. *J. Phys. Chem. Sol.* **45** (1984) 1175.
- Lunkenheimer, P. and Loidl, A. "Broadband Dielectric Spectroscopy", Ed.: F. Kremer and Schonhals (Springer-Verlag, Berlin, 2002), P.131.
- Lunkenheimer, P. and Loidl, A., *Phys. Rev. Lett.* **91** (2003) 207601.
- Mostafa, M.F and Elkhiyami, Sh., *J. Phys. Chem. Sol.* **188** (2018) 6.

(Received: 15 / 4 / 2018 ;  
accepted: 7 / 5 / 2018 )

## دراسة المعاوقة الطيفية والتغيرات الطورية لمركب عضوي- غير عضوي هجين جديد من هجائن القلويات الأرضية

مهجه فريد مصطفى ، أحمد كامل تمام و دينا سيد عبدالجواد  
قسم الفيزياء- جامعة القاهرة - الجيزة - مصر

المركب 1,7 هيبنتان ثنائي الأمونيوم رباعي كلوريد الكالسيوم – هجين جديد من المواد العضوية الغير عضوية- له تركيب جزيئي  $CaCl_4 [(CH_2)_7(NH_3)_2]$  يتبلور في تركيب فراغى احادى الميل مجموعة Pm مع أبعاد:

$$V= 641.2 \text{ \AA}^3, \gamma= 90^\circ, \beta= 86.82^\circ, \alpha= 90^\circ, c= 12.391 \text{ \AA}, b= 11.205 \text{ \AA}, a=4.625 \text{ \AA}$$

كثافته = 1.63 مغم م<sup>-3</sup> و Z=2.

أثبت المسح الجزئي الحراري لهذا المركب وجود خمس تغيرات طورية: إثنان عند درجتى حراره  $T_1=329.2 \text{ K}$  و  $T_2= 326.49 \text{ K}$  تمثلان تفكك السلسله العضويه بالإضافة إلى ثلاث تغيرات طورية عند درجات حراره  $T_3= 283.6 \text{ K}$  و  $T_4= 278.8 \text{ K}$  و  $T_5= 206.8 \text{ K}$  وهى مصاحبه لتغيرات من نوع (صلب إلى صلب). تم عمل قياسات ثابت العزل الكهربى و التوصيليه الكهربيه كدوال فى درجة الحراره فى المدى (170-425) كلفن ومدى الترددات (0.06-40) ك هرتز. أثبت سلوك التوصيليه الكهربيه أنها نشطه حرارياً. أمكن تقسيم اعتماد التوصيليه الكهربيه حرارياً إلى ثلاث مناطق مختلفه. تم تقسيم اعتماد طاقة التنشيط على التردد إلى منطقتين بحيث تكون طاقة التنشيط (1) بمدى (0.64-0.42)eV فى المدى (-355-423) كلفن و طاقة التنشيط (2) بمدى (0.42-1.75)eV فى المدى (261-243) كلفن على الترتيب. فى الطور الثالث تكون طاقة التنشيط  $10^{4-10} (4.44 \text{ eV})$  ولا تعتمد على التردد.